Macedonian Journal of Chemistry and Chemical Engineering, Vol. **40**, No. 2, pp. 197–211 (2021)

MJCCA9 – 830

ISSN 1857-5552
e-ISSN 1857-5625

Received: February 11, 2021
Accepted: June 7, 2021

DOI: 10.20450/mjcce.2021.2396
Original scientific paper

INVESTIGATING STRUCTURAL CHANGES OF CHITOSAN-TiO_2 AND CHITOSAN-TiO_2-ZnO-MgO HYBRID FILMS DURING STORAGE BY FTIR SPECTROSCOPY

Luis M. Anaya-Esparza[1,2], José M. Ruvalcaba-Gómez[3], Rafael Romero-Toledo[2], Jorge A. Sánchez Burgos[1], Efigenia Montalvo-González[1*], Alejandro Pérez-Larios[2*]

[1]*Laboratorio Integral de Investigación en Alimentos, Tecnológico Nacional de México/Instituto Tecnológico de Tepic. Av. Tecnológico 2595 Fracc. Lagos del Country, Tepic 63175, México*
[2]*Laboratorio de Investigación en Materiales, Agua y Energía, Departamento de Ingenierías, Centro Universitario de los Altos, Universidad de Guadalajara, Av. Rafael Casillas Aceves 1200, Tepatitlán de Morelos 47600, México*
[3]*Campo Experimental Centro Altos de Jalisco, Instituto Nacional de Investigaciones Forestales, Agrícolas y Pecuarias, Boulevard de la Biodiversidad 2470, Tepatitlán de Morelos 47600, México*
*These authors contributed equally to the direction of this work

emontalvo@ittepic.edu.mx; alarios@cualtos.udg.mx

This work aimed to evaluate the effect of time and two storage temperatures (25 °C and 4 °C) on the structural changes in chitosan (CS) films functionalized with titanium dioxide (TiO_2) and a ternary mixed oxide-based TiO_2 (TiO_2-ZnO-MgO; TZM) by Fourier transform infrared (FTIR) spectroscopy and the *in vitro* release of TiO_2 and TZM from the CS film to the medium. Changes in the FTIR spectra (mainly in the 1700 to 1250 cm^{-1} region) of the CS-based films during storage were dependent on the storage temperature. The film stored at 25 °C showed remarkable changes after 7 days of evaluation, indicating a dehydration process; however, films stored at 4 °C exhibited reduced changes after 21 days of storage. Moreover, the migration behavior of TiO_2 (< 13%) and TZM (< 7%) from CS to the medium showed a first-order kinetic model ($R^2 > 0.93$) in a temperature-dependent response. Further studies are needed to correlate the structural changes of CSTiO_2 and CSTZM films during storage with their technological and functional properties, which could limit their potential applications.

Keywords: functionalization; chitosan film; titanium dioxide; structural changes; storage

ИСТРАЖУВАЊЕ НА СТРУКТУРНИ ПРОМЕНИ НА ХИБРИДНИ ФИЛМОВИ ОД ХИТОЗАН-TiO_2 И ХИТОЗАН-TiO_2-ZnO-MgO ПРИ СКЛАДИРАЊЕ СО ПОМОШ НА FTIR-СПЕКТРОСКОПИЈА

Целта на овој труд е да се процени влијанието на време и на две температури на складирање (25 °C and 4 °C) врз структурните промени на филмови од хитозан (CS) функционализирани со титаниум диоксид (TiO_2) и тројни мешани оксиди на основа на TiO_2 (TiO_2-ZnO-MgO; TZM) со Фуриеова трансформна инфрацрвена (FTIR) спектроскопија и *in vitro* ослободување на TiO_2 и TZM од медиумот на филмот од CS. Промените на FTIR-спектрите (главно во областа од 1700 до 1250 cm^{-1}) на филмовите базирани на CS за време на складирање беа зависни од температурата на складирањето. Филмот складиран на 25 °C покажуваше значајни промени по 7 дена од проценувањето, укажувајќи на процес на дехидратација. Меѓутоа, филмовите чувани на 4 °C покажаа намалени промени по 21 ден од складирањето. Освен тоа, миграциското однесување на TiO_2 (< 13%) и TZM (< 7%) од CS кон медиумот покажува на кинетички модел од прв ред ($R^2 >$ 0,93) во температурно зависен одговор. Потребни се понатамошни испитувања на корелацијата на структурните промени на филмовите на CSTiO_2 и CSTZM за време на складирање со нивните технолошки и функционални својства, кои би можеле да ја ограничат нивната потенцијална употреба.

Клучни зборови: функционализација; филм од хитозан; титаниум диоксид; структурни промени; складирање

1. INTRODUCTION

There is an enormous demand for hybrid materials in recent years because of their excellent chemical and physical properties for several industrial and biomedical applications [1, 2]. Hybrid composites consist of a combination of two or more inorganic and organic compounds (inorganic/inorganic, organic/organic, or inorganic/organic) through covalent or non-covalent interactions, which can be prepared by different synthesis methods, such as sol-gel, hydrothermal, precipitation, self-assembly, dispersion-assembly, nanobuilding blocks, and intercalation [2, 3]. Functionalization is a viable strategy applied to modify the technological properties of hybrid materials, mainly organic/inorganic composites [1, 4]. Currently, special attention has focused on the functionalization of natural polymers (carboxymethyl cellulose, starch, gums, and chitosan) with inorganic (metallic or transition metal compounds) nanoparticles to obtain hybrid composites [4], particularly for the chitosan-TiO_2 based hybrid composites [5].

Chitosan is a versatile biopolymer obtained after deacetylation of chitin and constituted by β-(1–4)-linked D-glucosamine and *N*-acetyl-D-glucosamine [6]; moreover, due to its properties (cationic character, soluble in organic acids, non-toxic, biodegradable, and biocompatible with antimicrobial activity and film-forming ability), it is considered a functional compound widely applied in biotechnology, engineering, water treatment, food preservation, agriculture, and medicine [2, 5–8]. Furthermore, chitosan has functional groups ($–NH_2$ and –OH), which can react with compounds like TiO_2 nanoparticles to improve its technological properties and applicability [5].

Titanium dioxide (TiO_2) is a multi-use and compatible material with relevant industrial and environmental uses [9], mainly due to its antimicrobial properties [10]. It has been used as a surface sanitizer (medical, pharmaceutical, and food applications) [11] as well as for water treatment [12]. Furthermore, TiO_2 is widely employed as an additive in the pharmaceutical and food industries as a white pigment [13]. Nonetheless, recently, TiO_2 has been used as a reinforcement agent of protein [1] and polysaccharide-based composites [4], including chitosan (CS-TiO_2) [5], to improve its physicochemical and mechanical properties with diversified applications.

The CS-TiO_2 hybrid material exhibits good antimicrobial activity against bacteria, yeast, and mold [14, 15], and photocatalytic activity for the degradation of different water pollutants (2,4-dichlorophenol, methyl orange, and methylene blue) and the removal of heavy metals (Cd(II), As(III), Cr(VI), Ni, Cu, and Hg) [16–20]. Furthermore, CS-TiO_2 has shown interesting biomedical applications, mainly for the development of wound healing materials [12], drug delivery systems [21], and biosensors [22]. In the food industry, CS-TiO_2 has been used to develop packaging materials for fruit preservation [23, 24], which demonstrated ethylene degradation activity [15]. In general, the addition of TiO_2 improves the functionality and applicability of CS-based films; nonetheless, a higher functionality of CS-TiO_2 hybrid film properties was observed when nano-TiO_2 nanoparticles were previously functionalized with other compounds (i.e. CS-TiO_2:Cu or CS-TiO_2:Ag) [17, 25]. In this context, ternary mixed oxide-based TiO_2 (TiO_2-ZnO-MgO) displayed improved structural and textural properties, with higher antibacterial activity (against *Staphylococcus aureus, Salmonella paratyphi, Listeria monocytogenes,* and *Escherichia coli*) compared to TiO_2 and without toxic effects in *Artemia salina* [10, 26], which could be potentially used as a reinforcement agent of CS-based materials.

An essential factor that must be considered when establishing the feasibility of any polysaccharide-based film for diverse applications is the modification of its properties over time and as a function of storage temperature [27]. In this context, it has been reported that storage time and temperature negatively affected the mechanical and water-barrier properties of chitosan-based films [28] as well as their antimicrobial activity [29]. On the other hand, the characterization of CS-based films functionalized with TiO_2 and their interactions has been extensively evaluated by Fourier transform infrared (FTIR) studies [15, 19, 23, 30]. Although it has been shown that TiO_2 (doped or undoped) promotes changes in the CS-based film structure (at the time of fabrication), thereby enhancing its technological and functional properties [5], studies about the effect of storage conditions (time and temperature) on the structural changes in CS-TiO_2 hybrid materials are scarce. Therefore, the objective of this work was to evaluate the effect of time and two storage conditions

(ambient storage at 25 °C and refrigerated storage at 4 °C) on the structural changes in CS-TiO_2 and CS-TiO_2-ZnO-MgO hybrid films by FTIR studies as well as the *in vitro* release of TiO_2 and TZM from the CS matrix to the medium at two temperatures.

2. EXPERIMENTAL SECTION

2.1. *Preparation of chitosan-TiO_2-ZnO-MgO hybrid films*

The hybrid films were manufactured using the evaporative casting method according to Yong et al. [31] with some modifications. The chitosan (CS, medium molecular weight, Sigma Aldrich Chemical Company, St. Louis, MO, USA) film-forming solution was prepared by dissolving 1 g of CS in 95 ml of 1 % acetic acid solution under continuous magnetic stirring at 25 °C. Then, the pH of the solution was adjusted to 4.8 using NaOH (1 M) [32]. Subsequently, TiO_2 or TiO_2-ZnO-MgO (TZM, containing 5 % Zn and 5 % Mg) mixed oxide (at 500 μg ml^{-1}) nanoparticles [10, 26] were added to the CS solution. The nanoparticles were previously dissolved in 5 ml of 1 % acetic acid solution and sonicated (Fisherbrand™, CPX1800 Ultrasonic bath, Branson Korea Co., Ltd. South Korea) for 5 min to avoid agglomerations. Afterward, glycerol (15 % by weight of total solids) was added with continuous magnetic stirring for 20 min on the film-forming solution. The resultant solution was then deposited onto a Petri dish (100*15 mm) and allowed to dry at 37 °C for 24 h. A pure CS film was used as a control. Hybrid films were labeled as CSTiO_2 (chitosan + TiO_2 at 500 μg/ml) and CSTZM (chitosan + TZM at 500 μg/ml). In general, TiO_2 and TZM nanoparticles have a semi-globular form with a polycrystalline nature and an anatase phase with a mean particle size in the range of 18.255 nm and 23.25 nm, respectively [10, 26].

2.2. *Film thickness and moisture content*

The thickness of the CS-based films was determined using a manual digital micrometer (Digimatic micrometer, 0.001 mm, Mitutoyo Co., Kobe, Japan). The film thickness was measured on average in at least ten measurements from 5 random locations on each film sample [33]. Additionally, the moisture content of the CS-based films was determined by drying the sample (9 cm^2 film) at 110 °C to a constant weight (by triplicate) [31]. The moisture content was calculated using the following equation (1):

$$\text{Moisture content (\%)} = [(M_i - M_f)/(M_i)] \cdot 100, \quad (1)$$

where M_i and M_f are the initial and final weights of the sample, respectively.

2.3. *Fourier transform infrared (FTIR) spectroscopy analysis*

The FTIR spectrum for the films was examined with an attenuated total reflectance FTIR spectrometer (Nicolet iS5, ThermoFisher Scientific, Tokyo, Japan). The spectrum was recorded at room temperature (25 ± 1 °C) in the range from 4000 to 400 cm^{-1} with 24 scans and a resolution of 4 cm^{-1}. A background scan was recorded before the measurement and subtracted for the sample spectra. The FTIR spectra were normalized to the same area and compared to each other. Deconvolution of this spectral region into Gaussian components was performed to separate overlapping peaks in the region between 1700 and 1250 cm^{-1} [34]. Deconvolution was also used to estimate the area related to the specific vibration of each selected peak [35]. Samples were analyzed by duplicate in two different film points at 1, 7, 14, 21, and 28 days. All data manipulation was carried out using Origin® software (OriginLab Corporation v. 2016).

2.4. *In vitro release of TiO_2 from the chitosan matrix to the medium*

The *in vitro* release of TiO_2 and TZM nanoparticles from the chitosan matrix to the medium (phosphate buffer with pH 7.0 at 25 °C or 4 °C) was evaluated using a static Franz diffusion cell system (Fig. 1). The film was cut into small circles (diameter of 125 mm) and used as a membrane in the static system. The release of TiO_2 and TZM from the polymeric matrix was measured using a spectrophotometer (Shimadzu UV-2600, Tokyo, Japan) at a wavelength from 500 to 200 nm at 0.5, 1, 2, 4, 6, 12, and 24 h [36]. A first kinetic mathematical model was employed to evaluate the TiO_2 and TZM release from the film to the medium, as suggested by Timotius et al. [36]. The concentration of TiO_2 or TZM was calculated using a calibration curve of pure TiO_2 (0, 50, 100, 250, and 750 μg/ml) at 400 nm [13].

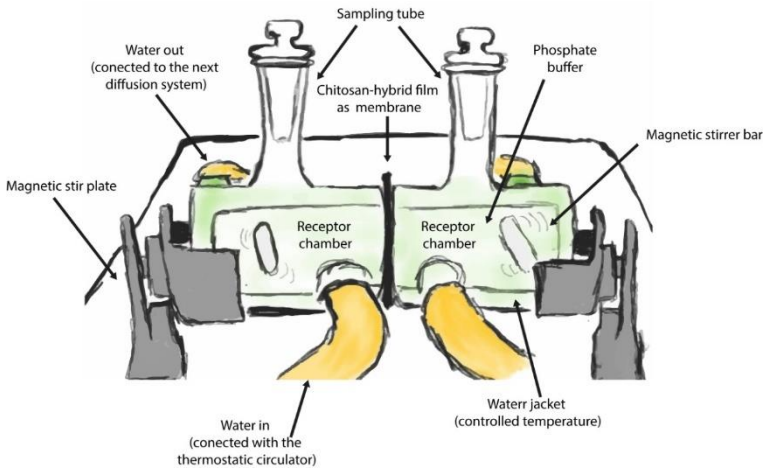

Fig. 1. Schematic diagram of the static Franz diffusion cell system for in vitro release of TiO_2 from the chitosan matrix to the medium

2.5. *Data analysis*

The thickness and moisture content data were subjected to the analysis of variance (One-way ANOVA, $\alpha = 0.05$) and Tukey test ($p < 0.05$). Multivariate analysis was applied for the interpretation of structural changes. Principal component analysis (PCA correlation matrix) was used to determine patterns in the structural changes and to evaluate their relationship with the storage time and temperature. Components were calculated without rotation, and the number of extracted factors was based on eigenvalues (> 1.0) and explained variance (> 70 %). All data were analyzed by the Statistica software (V.12.5 Statsoft®, Tulsa, USA).

3. RESULTS AND DISCUSSION

Figure 2 shows the appearance of chitosan-based films with or without the added TiO_2 and TZM nanoparticles after 28 days of evaluation at two storage conditions (25 and 4 °C). The CS film was flexible and transparent on the preparation day (Fig. 2a); however, after 28 days of storage, visible changes in the film were observed, mainly at ambient conditions where the film was rigid and looked dehydrated with a yellow tone (Fig. 2b) compared to the CS film stored at 4 °C (Fig. 2c), where minimum changes were appreciated compared to the 1-day film.

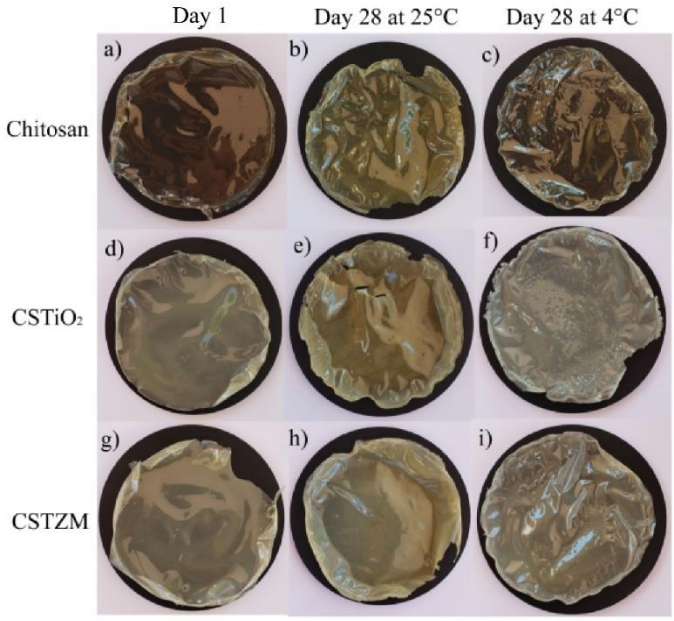

Fig. 2. Appearance of chitosan films (a–c), chitosan films functionalized with TiO_2 nanoparticles ($CSTiO_2$, d–e), and chitosan films functionalized with TiO_2-ZnO-MgO nanoparticles (CSTZM, g–i). The films were stored at ambient (25 ºC) and refrigerated temperatures (4 ºC).

Similar trends were observed in the films functionalized with TiO_2 (Figure 2d–f) and TZM (Fig. 2g–i) in the experimental conditions evaluated. The $CSTiO_2$ and CSTZM films in ambient temperature were rigid and brittle at the end of storage, while the refrigerated films were flexible with minimum changes perceived in appearance. Fernández-Saiz et al. [29] mentioned that color changes in chitosan films stored at 37 °C (from colorless to yellowness) are a visible indicator of chemical alterations in the biomaterial. The main changes in the CS-based films with or without the added nanoparticles and stored at 25 °C could be attributed to the loss of water molecules by a dehydration process [37].

Table 1 lists the average thickness of the chitosan films with and without the added nanoparticles. A significant increase ($p < 0.05$) of the CS film thickness (79.83 μm) was observed by the incorporation of TiO_2 (102.08 μm) and TZM (101.16 μm). These results are in line with previous reports for the thickness of chitosan films functionalized with TiO_2, increasing from 70 to 116 μm in a TiO_2-concentration dependence (from 2 to 6 mg/ml) [38].

T a b l e 1

Experimental matrix and average thickness of chitosan-based films

Treatments (code)	Film sample	NPs concentration (μg/ml)	Thickness film (μm)
CS	Chitosan	0	79.83 ± 4.30^{b}
$CSTiO_2$	Chitosan + TiO_2	500	102.08 ± 2.23^{a}
CSTZM	Chitosan + TiO_2-ZnO-MgO	500	101.16 ± 2.24^{a}

Values are the average ± standard deviation ($n = 10$). Different letters (a or b) in each column indicate statistically significant differences between treatments ($p < 0.05$). Chitosan films functionalized with TiO_2 nanoparticles ($CSTiO_2$). Chitosan films functionalized with TiO_2-ZnO-MgO (CSTZM). NPs: Concentration of TiO_2 or TZM nanoparticles.

The moisture content of the CS-based films with and without the added nanoparticles after 28 days of ambient and cold storage are given in Table 2. A significant decrease ($p < 0.05$) in the moisture content of the CS-based film (13.26 %) was observed due to the incorporation of TiO_2 (9.81 %) and TZM (10.98 %) on the first day. These results agree with those reported in a chitosan-starch film when TiO_2 was added [39], which is associated with the mesoporous character and absorptive properties of TiO_2 [33]. On the other hand, the CS-based films exhibited loss in the moisture content during storage ($p < 0.05$). The moisture of the CS film after 25 days of storage at 25 °C decreased from 13.26 % to 3.77 %, while at 4 °C, it decreased up to 8 %, indicating that cold temperatures can help to retard the loss of moisture content in the CS film [28]. Meanwhile, the $CSTiO_2$ (from 9.81 % to 4.17 % or 8.24 %) and CSTZM (from 10.98 % to 4.13 % or 8.21 %) films exhibited a similar moisture content independent of storage conditions (25 °C and 4 °C, respectively), with a lower moisture loss at ambient temperature (57 % and 62 %, respectively) than the CS film (71 %). The addition of TiO_2 or TZM into the CS film may retard the dehydration process due to their ability to participate in hydrogen bonding with CS [38]; however, this effect depends on the storage conditions.

T a b l e 2

Moisture content of chitosan-based films after storage

Treatments	Moisture content (%)		
	Day 1	Storage at 25 °C (day 28)	Storage at 4 °C (day 28)
CS	13.26 ± 0.22^{aZ}	3.77 ± 0.46^{aY}	8.00 ± 0.08^{cX}
$CSTiO_2$	9.81 ± 0.13^{cZ}	4.17 ± 0.19^{aY}	8.24 ± 0.08^{aX}
CSTZM	10.98 ± 0.33^{bZ}	4.13 ± 0.25^{aY}	8.21 ± 0.09^{abX}

Values are the average ± standard deviation ($n = 3$). Lowercase letters (a, b, or c) in each column indicate statistically significant differences between treatments ($p < 0.05$). Capital letters (X, Y, or Z) in each row indicate statistically significant differences between storage time ($p < 0.05$). NPs: Concentration of TiO_2 or TZM nanoparticles.

3.1. *FTIR characterization of CS-based films*

FTIR spectroscopy is a tool that provides information through band properties, frequencies, and intensities, which permits the structural changes in CS-based films promoted by storage conditions to be studied [40]. Figure 3 shows the FTIR spectra of a CS (Figure 3a,b) film functionalized with TiO_2 (Figure 3c,d) and TZM (Figure 3e,f) nanoparticles stored at ambient and cold storage conditions. CS-films with or without TiO_2 or TZM nanoparticles exhibited similar spectra profiles, consistent with previous reports [39, 41]. The broad absorption peaks around 3500–3000 cm^{-1} (centered at 3300 cm^{-1}) were ascribed to stretching vibrations of overlapping –OH and N–H groups through the saccharide ring of the CS structure [40], while the weak peaks at 2933 cm^{-1} and 2869 cm^{-1} corresponded to the stretching modes of the C–H bond of the methylene functional group [40]. The peaks around 1650 cm^{-1} and 1556 cm^{-1} were assigned to amide I and amide II vibrations [41], both attributed to the NH^{3+} groups by the effects of protonation during film development in an acetic acid solution leading to the formation of the amide bond (–N–C=O) [29]. Furthermore, the peaks at 1414 cm^{-1}, 1379 cm^{-1}, and 1323 cm^{-1} were ascribed to the stretching vibration of $–CH_2$ bending, $–CH_3$ symmetrical deformation, and C–N band, respectively [39]. The bands from 1091 cm^{-1} (C–O stretching at C3), 11027 cm^{-1} (C–O stretching at C6), and 915 cm^{-1} were due to the C–O–C stretching from glycosidic bonds [41]. The peak around 844 cm^{-1} corresponds to the wagging (C–H) of the saccharide nature of chitosan [42].

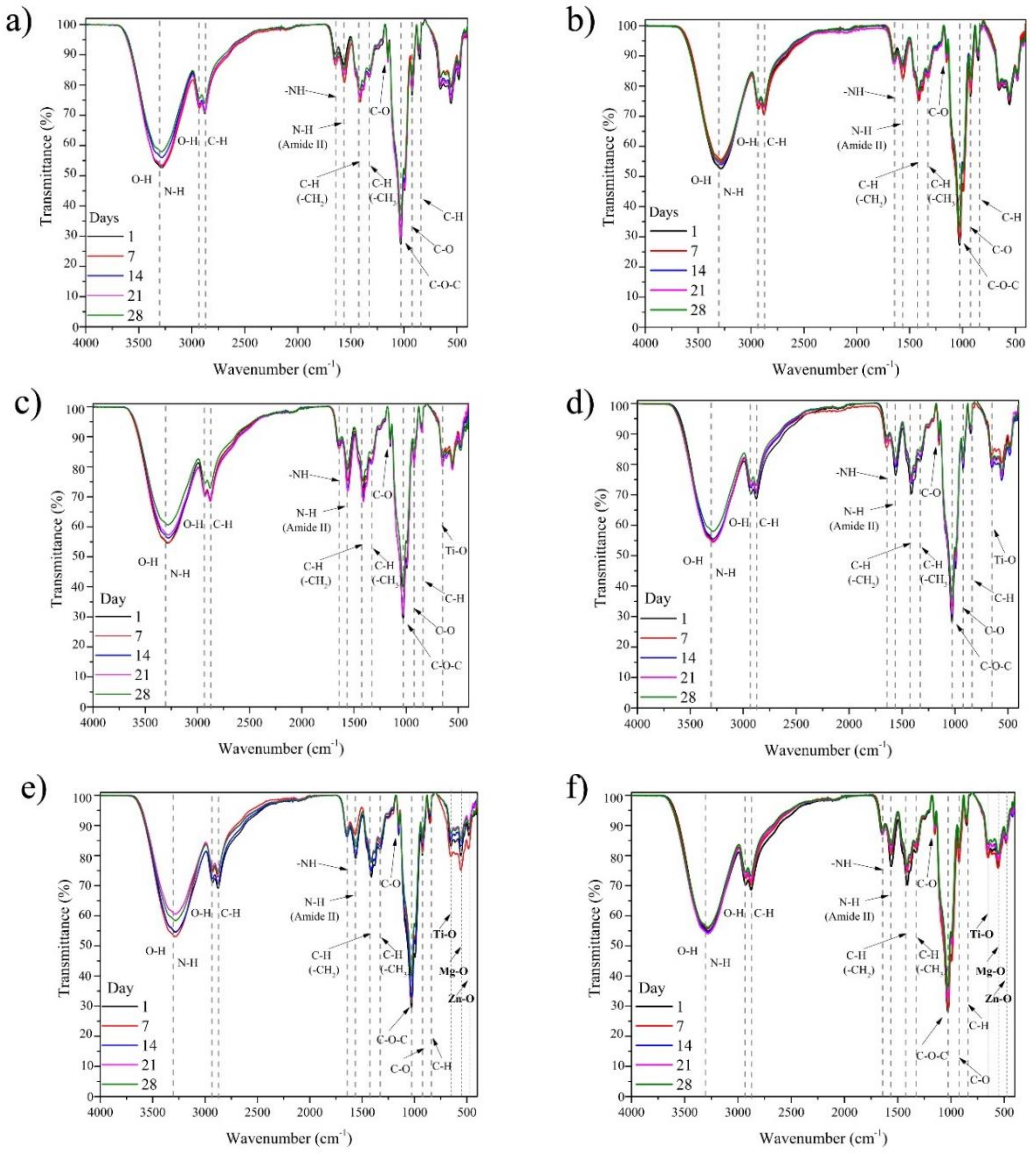

Fig. 3. FTIR spectra of chitosan films (a, b), chitosan films functionalized with TiO_2 nanoparticles (c, d), and chitosan films functionalized with TiO_2-ZnO-MgO nanoparticles (e, f) when the films were stored at 25 ºC (a, c, e) and 4 ºC (b, d, f)

Concerning the $CSTiO_2$ and CSTZM films, they exhibited a similar spectra compared with CS film. It has been previously reported that the incorporation of TiO_2:Ag-doped nanoparticles into a chitosan film did not alter the characteristic FTIR spectra of CS and exhibited a similar profile to a CS-TiO_2 hybrid film [40]. The interaction of CS with TiO_2 during the formation of the organic-inorganic complex occurs in the amorphous region of chitosan through the hydrogen bond formation at 3300 cm^{-1} ($–NH_2$) [15]. Moreover, stretching vibrations of C–O and –OH groups at 2933 cm^{-1} are strongly attached to the TiO_2 and TZM nanoparticles, promoting electrostatic interactions between organic and inorganic compounds to form the hybrid composite [19]. On the other hand, a displacement in the CS spectra by incorporation of TiO_2 and TZM was observed in the region from 1700 to 400 cm^{-1}, in particular, from 1650 to 1642 cm^{-1}, from 1566 to 1561 cm^{-1}, and from 1414 to 1409 cm^{-1} due to amine I, amide II, and N–H bending vibrations, respectively (Fig. 4) [43]. Similar trends were reported by Zhang et al. [43] by adding TiO_2 in a CS film; they reported a shift of 23 cm^{-1} (from 1636 to 1615 cm^{-1}), indicating the interaction between TiO_2 and TZM nanoparticles take place at the amine site of CS. Likewise, a decrease in the intensity of the peak centered at 1029 cm^{-1} of the CS-based films by incorporation of TiO_2 and TZM was detected, suggesting the formation of the Ti–OH bond at the OH group of CS [42, 44, 45]. Furthermore, some peaks at 649 cm^{-1}, 614 cm^{-1}, 553 cm^{-1}, 482 cm^{-1}, and 414 cm^{-1} were observed in the functionalized CS-based films (Fig. 4), which were related to Ti–O bonds, indicating the interaction of TiO_2 with CS ($CSTiO_2$) [10, 46, 43]. Furthermore, the signals in the CSTZM film may be related to Ti–O, Zn–O, Mg–O, Ti–O–Ti, Ti–O–Zn, Ti–O–Mg, or Zn–O–Mg bonds, which could interact with the CS structure (through electrostatic interactions) to form the hybrid film, suggesting that the TZM mixed oxide were embedded in the surface of the CS-based film [30, 47, 48, 49]. Signals around 655 cm^{-1}, 565 cm^{-1}, and 465 cm^{-1} were detected in a CS film functionalized with Ti/ZnO, TiO_2, ZnO, and SiO_x nanoparticles, which are attributed to the Ti–O, Zn–O, and Si–O bonds [50]. Malhorta and Kaushik [51] suggested that changes in these regions on the hybrid composite indicate the immobilization of inorganic nanoparticles on the chitosan matrix. Furthermore, on day 7, the CSTZM film stored at ambient temperature increased its intensity in the region of 750 to 400 cm^{-1} (Fig. 3e). The increase in intensity implies the increase in the number of free ions in the polymeric matrix due to the magnesium dissociation, which is present in the ternary mixed oxide system [52].

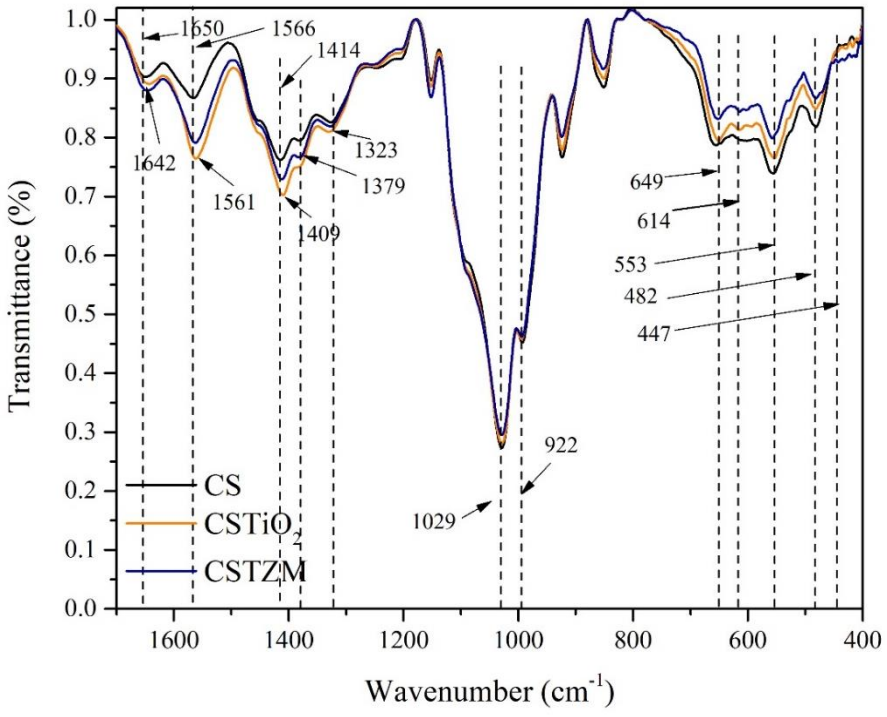

Fig. 4. FTIR spectra of chitosan films (CS), chitosan films functionalized with TiO_2 nanoparticles ($CSTiO_2$), and chitosan films functionalized with TiO_2-ZnO-MgO nanoparticles (CSTZM) in the region of 1700 to 400 cm^{-1}

3.2. *Effect of storage conditions on CS-based films*

Concerning the storage conditions, the CS-based films with or without the added nanoparticles exhibited changes in the transmittance values promoted by time and temperature (Fig. 5). On day 28, the CS film stored at 25 °C exhibited changes in the transmittance values (from 52 to 57 %) in the region of 3500–3000 cm^{-1} in a time-dependent response (from 1 to 28 days) compared to the film stored at 4 °C (from 52 to 55 %), which was attributed to the amine dehydration and the loss of water molecules as a consequence of the storage temperature [34]. Moreover, peaks at 1652 cm^{-1} (from 90 to 87 %) and 1569 cm^{-1} (from 86 to 82 %) showed decreased transmittance values for the CS film at 25 °C compared to the CS film stored at 4 °C (from 90 to 88 % and from 87 to 86 %, respectively). These variations were associated with changes in the acetyl group of the CS structure by the influence of a dehydration/hydration process [34]. Similar trends were reported in an alginate film due to water evaporation using ATR-FTIR spectroscopy [44].

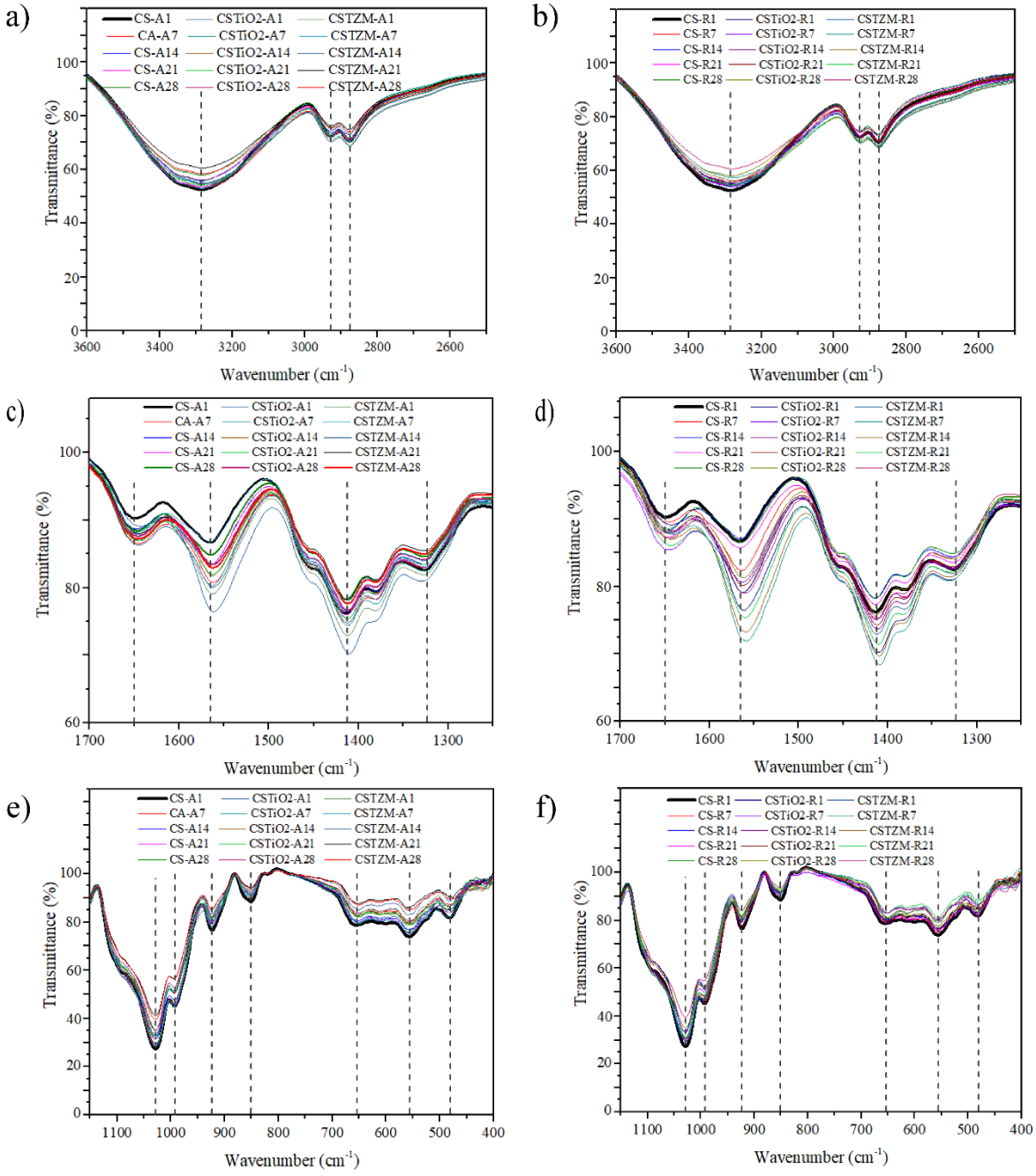

Fig. 5. FTIR spectra of CS-based films by regions (3600–2500 cm^{-1}, 1700–1250 cm^{-1}, and 1150–400 cm^{-1}) and their changes due to the effect of storage at 25 ºC (a, c, e) and 4 ºC (b, d, f)

Despite the fact that the CS, $CSTiO_2$, and CSTZM films exhibited similar FTIR spectra (Figs. 3a-f), the main changes observed during storage of the CS-based films (CS, $CSTiO_2$, and CSTZM) were in the region of 1700 to 1250 cm^{-1} (Figs. 5a-f) for both storage temperatures [34, 53]. These results agree with those reported by Kam et al. [53], who evaluated the effect of storage conditions (3 weeks stored at 28 °C and 4 °C) on the chitosan film structure and reported qualitative differences in the FTIR spectra of CS films after three weeks of storage (28 °C and 4 °C), mainly in the region from 1655 cm^{-1} to 1565 cm^{-1}. According to Kaewklin and Siripatrawan [23], changes in the FTIR spectral profile are related to a matrix alteration promoted by environmental conditions.

A deconvolution process in the Gaussian components was performed to quantify the changes observed in the spectra of the CS-based films in the region from 1700 to 1250 cm^{-1}, as suggested by Mejenom et al. [54], who investigated the structural changes of chitosan by the incorporation of ammonium bromide in the FTIR spectral range from 1750 to 1450 cm^{-1}. Moreover, the deconvolution technique has been applied to investigate the role of the –OH and –NH vibrational groups in chitosan-montmorillonite composites in the region from 3600 to 2800 cm^{-1} by FTIR studies [34]. Table 3 lists the values of the central frequencies of the Gaussian components together with the integrated areas of the CS, $CSTiO_2$, and CSTZM films stored at ambient and refrigerated temperatures and their related changes during storage, considering the day of preparation as day one and the end of storage as day 28.

T a b l e 3

List of peak frequencies and integrated areas of the deconvoluted bands in the region 1700–1250 cm^{-1} for the chitosan-based films

Film		Ambient storage (25 °C)				Refrigerated storage (4 °C)	
		Day 1		Day 28		Day 28	
		Peak (cm^{-1})	Area (%)	Peak (cm^{-1})	Area (%)	Peak (cm^{-1})	Area (%)
CS	A	1649.15	7.43	1647.92	10.13	1648.94	12.22
	B	1569.70	17.83	1567.77	22.75	1566.91	20.28
	C	1458.75	11.65	1458.45	10.42	1458.53	10.71
	D	1415.99	19.26	1415.29	19.83	1415.51	16.11
	E	1378.13	3.29	1377.93	4.35	1378.43	2.87
	F	1338.57	40.49	1336.05	32.49	1337.25	37.79
$CSTiO_2$	A	1643.92	7.13	1646.04	11.02	1645.71	9.91
	B	1558.53	26.37	1562.91	22.66	1561.48	25.52
	C	1448.99	17.43	1457.82	10.89	1455.96	11.92
	D	1409.41	13.76	1413.79	20.62	1412.68	18.75
	E	1377.80	4.08	1377.24	3.87	1377.65	4.22
	F	1338.79	31.20	1336.78	30.91	1336.80	29.65
CSTZM	A	1645.89	8.36	1645.48	12.06	1644.32	9.51
	B	1562.23	25.47	1562.53	24.35	1559.05	28.61
	C	1453.93	9.13	1457.59	10.37	1452.05	13.89
	D	1412.06	17.59	1413.31	21.19	1410.70	16.21
	E	1377.84	4.83	1376.78	4.47	1377.85	4.85
	F	1336.49	30.08	1334.99	27.53	1336.64	26.91

CS = Chitosan. $CSTiO_2$ = Chitosan + TiO_2. CSTZM = Chitosan + TiO_2-ZnO-MgO

The deconvolution technique provides additional information about specific changes in the polysaccharide structure promoted by environmental conditions [34]. By deconvolution of the area band between 1700 and 1250 cm^{-1}, six components (A to F) were observed for the CS, $CSTiO_2$, and CSTZM films. Lawrie et al. [55] reported that the 1800–1200 cm^{-1} region of the CS deconvoluted spectra generates five components. In general, the integrated area in components A to F of the CS-based films with or without the added nanoparticles was influenced by the storage conditions.

After 28 days of storage, an increase in the integrated area of the components A (1649 cm^{-1})

and B (1569 cm^{-1}) of the CS film was observed in both ambient (10.13 and 22.75 %, respectively) and refrigerated (12.22 and 20.28 %, respectively) storage in comparison with the film on the first day (7.43 %). Branca et al. [34] argued that the area increase in these regions is due to a dehydration/hydration process with a progressive weakening of the hydrogen bond that involves the loss of water molecules. This phenomenon affects the –CH stretching band, amide I, and amide II of the CS structure, which are sensitive to the formation/rupture of hydrogen bonds [56]. Component C (at 1458 cm^{-1}, area of 11.65 %) and D (at 1415 cm^{-1}, area of 19.26 %) did not show significant changes throughout the storage period at ambient (10.42 and 19.83 %, respectively) and refrigerated (10.71 and 16.11 %, respectively) temperatures. Components E (1378 cm^{-1}) and F (1338 cm^{-1}) exhibited an area reduction at the end of storage in ambient (4.35 and 32.49 %, respectively) and refrigerated (2.87 and 37.79 %, respectively) temperatures compared to the film on the first day (3.29 and 40.49 %, respectively), which is associated with a partial breakage of the intramolecular and intermolecular interactions in the CH_3 group (at 1378 cm^{-1}) as a consequence of the storage conditions [57, 58].

In general, the CSTiO_2 and CSTZM films showed a displacement in the peak location (average of 10 cm^{-1}) of components A to D compared to the CS film on the first day. Furthermore, changes in the integrated area of the CS films were observed due to the functionalization with TiO_2 and TZM, with an increase in the A, B, C, and E components, while D and F decreased. Changes in the band intensity (mainly at 1405 cm^{-1}) after incorporation of TiO_2 and TZM could be associated with changes in the carboxylate group ($–NH_3^+–OOCH$). Furthermore, the addition of TiO_2 and TZM nanoparticles promotes superficial hydrophobic changes in the chitosan matrix [29].

The CSTiO_2 film (7.13 %) exhibited an increase in the integrated area of component A (1643 cm^{-1}) after 28 days of storage at ambient (11.02 %) and refrigerated (9.91 %) temperatures. Rivero et al. [56], in a deconvoluted CS film spectrum, found an increase in the peak located at 1635 cm^{-1}, which suggested that the inorganic filler was chemically bonded to the polymeric matrix. Component B (at 1558 cm^{-1}, area of 26.37 %) exhibited a decrease in the integrated area compared to ambient (22.66 %) and refrigerated (25.52 %) storage after 28 days of evaluation. A reduction in the area of component B could be associated with TiO_2, which may act as an anti-plasticizer agent absorbing the available water molecules in the film, promoting dehydration of the polymeric matrix during ambient storage [59]. This phenomenon is significantly lower during refrigerated storage, mainly by environmental humidity [29]. On the other hand, component C (at 1448 cm^{-1}, area of 17.43 %) showed a decrease (10.89 and 11.92 %, respectively); moreover, component D (at 1409 cm^{-1}, area of 13.76%) showed an increase in the integrated area after storage at ambient (20.62 %) and refrigerated (18.75 %) temperatures. These variations were associated with changes in the C–H functional group as a result of the storage conditions [56]. Yamamoto et al. [60] suggested that conformational changes promoted by water loss during storage could exist. Moreover, components E (4.08 %) and F (31.20 %) did not show significant changes due to the storage conditions (ambient: 3.87 and 30.91 %, refrigerated temperature: 4.22 and 29.65 %, respectively), associated with possible interactions between the C–H group of CS and the TiO_2 nanoparticles that provide higher stabilization of the carboxylate group than the CS film, thereby retarding the hybrid film dehydration process [61, 62].

Similar trends were observed in the integrated area of CSTZM to that reported for the CSTiO_2 film, which was attributed to the amount of TiO_2 (90% w/w) present in the ternary (TZM) mixed oxide system [10]. Component A (at 1645 cm^{-1}) showed an increase in the integrated area (8.36 %) after 28 days of storage at ambient (12.06 %) and refrigerated (9.51 %) temperatures. On the other hand, component B (at 1562 cm^{-1}) decreased when stored at ambient temperature (24.35 %) but increased during storage in refrigeration (28.61 %). Furthermore, components C (at 1453 cm^{-1}) and D (at 1412 cm^{-1}) showed an increase in the integrated area (9.13 and 17.59 %, respectively), while component E (1377 cm^{-1}) did not show significant changes. However, component F (1336 cm^{-1}) also exhibited a reduction in the integrated area of approximately 3 % in both ambient and refrigerated storage. These variations could be related to changes in the chitosan structure promoted by the storage conditions [56, 60].

Additionally, a multivariate statistical tool like principal component analysis (PCA) was used to estimate the interrelationship among CS-films and their changes promoted by the storage conditions. PCA has been employed for biopolymer characterization [63]. Figure 6 shows the total variance of 88 % that was explained in the first two principal components (65.32 % for PC1 and 22.90 % for PC2).

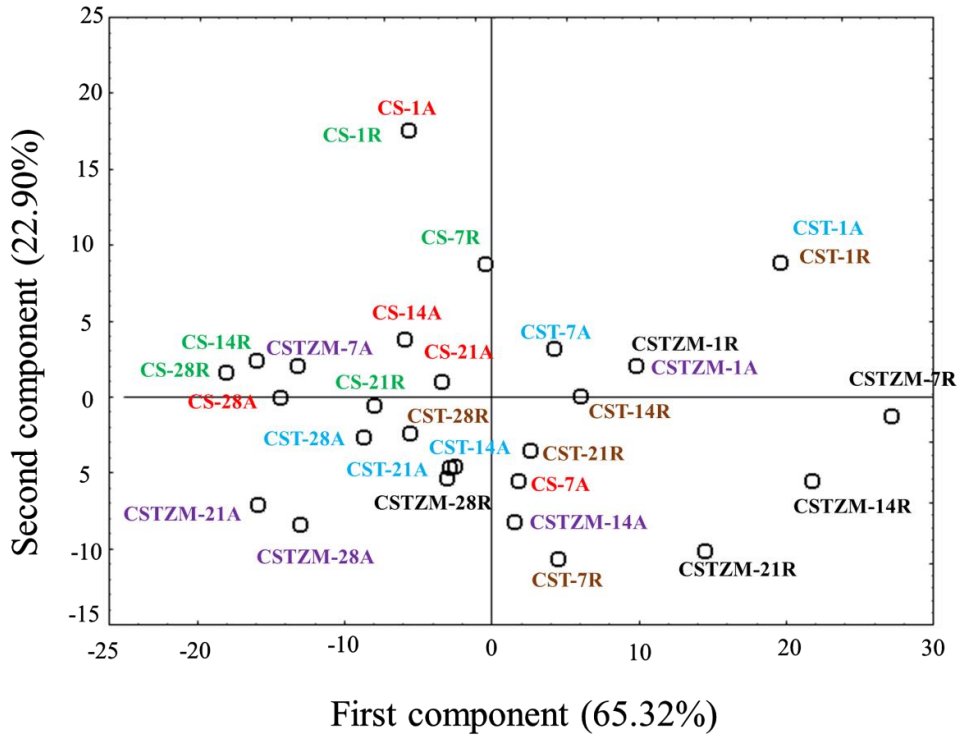

Fig. 6. Principal component scatters plot of FTIR spectra from CS-based films and their related changes promoted by the storage conditions. CS = Chitosan. CST = Chitosan + TiO_2. CSTZM = Chitosan + TiO_2-ZnO-MgO. The numbers 1, 7, 14, 21, and 28 indicate the days of storage. A = ambient storage. R = refrigerated storage.

The main FTIR spectral (1700–1250 cm^{-1}) changes of the CS-based films (with or without the added nanoparticles) stored at ambient temperature occur in the first 14 days of storage (with a remarkable effect on day 7) and continue during the evaluated time, which were associated with a dehydration process [37]. On the other hand, the CS film stored at 4 °C exhibited reduced changes through the storage period compared to the film stored at ambient temperature. Kam et al. [53] argued that the interaction between acetate ion and the amino group (1565 cm^{-1}) of CS existed at day 1, but this interaction was less evident during ambient storage, indicating a loss of the acetic acid from the films during time of storage [64]. On the other hand, CS films functionalized with TiO_2 and TZM nanoparticles and stored at refrigerated temperatures showed a retarded dehydration process where the main changes occurred after 21 days of storage. Kerch and Korkhov [28] mentioned that low temperatures help to keep the structural properties of CS-based films. Nonetheless, TiO_2 and TZM nanoparticles can act as a reinforcement agent in the chitosan matrix, which may lead to a modification of the level of hydration in the hybrid film [4, 63].

3.3. *In vitro release of TiO_2 and TZM from chitosan matrix to the medium*

The use of TiO_2 as a reinforcement agent of polysaccharide-based materials to enhance its technological and functional properties for diversified applications has increased in the last several years, especially in the development of active packaging materials for food and non-food purposes [1, 4, 5, 15]. On the other hand, due to direct contact of the packaging materials, the possible liberation or migration of TiO_2 from the polymer matrix to the medium should be evaluated and quantified [65]. The kinetic profile of TiO_2 and TZM release from the chitosan matrix is presented in Figure 7, and their percentages of *in vitro* release are given in Table 4.

In general, the migration behavior of TiO_2 and TZM nanoparticles from a chitosan film at ambient and at refrigerated storage could be explained using a first-order kinetic model (R^2 > 0.93). These results agree with those by Timotius et al. [36], who reported that chitosan films functionalized with curcumin showed a controlled kinetic release in a concentration-dependent response (R^2 from 0.987 to 0.996).

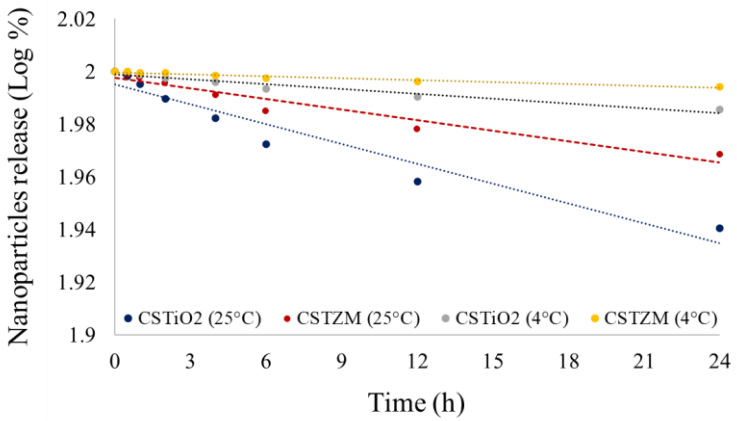

Fig. 7. First-order regression model for the release rate of TiO_2 and TZM nanoparticles from chitosan films functionalized with TiO_2 nanoparticles ($CSTiO_2$) and chitosan films functionalized with TiO_2-ZnO-MgO nanoparticles (CSTZM) at ambient (25 ºC) and refrigerated temperatures (4 ºC)

T a b l e 4

In vitro release of TiO_2 and TZM nanoparticles from the hybrid composite to the medium after 24 h of evaluation

Sample film	Temperature (°C)	Migration (%)	R^2
$CSTiO_2$	25	12.81	0.9396
CSTZM	25	7.00	0.9371
$CSTiO_2$	4	3.27	0.9502
CSTZM	4	1.30	0.9627

$CSTiO_2$ = Chitosan + TiO_2.
CSTZM = Chitosan + TiO_2-ZnO-MgO

In vitro release of TiO_2 and TZM from the chitosan matrix to the medium was also calculated according to the nanoparticles detected in the phosphate buffer solution after a defined evaluation time [65]. The migration ratio of the TiO_2 and TZM nanoparticles was dependent on the temperature evaluated. $CSTiO_2$ (12.81 %) and CSTZM (7 %) assessed at 25 °C exhibited higher release amounts compared to the samples assessed at refrigerated temperatures (3.27 and 1.30 %, respectively). These results could be attributed to the swelling properties and hydration rates of CS films, which may be influenced by the temperature [36]. Moreover, the release of TiO_2 and TZM nanoparticles includes the polymer degradation or surface erosion, promoting a higher level of migrated particles [66]. Lian et al. [64] reported 5.4 % migrated TiO_2 nanoparticles from a PVA-CS-TiO_2 film in a food simulant system after 11 h of evaluation. Likewise, Alizadeh-Sani et al. [67] observed that a low amount of TiO_2 was detected in a meat product coated with a whey protein isolate-cellulose-TiO_2 film. However, the detected amount of TiO_2 (< 1 % of the total food weight) followed the recommended safe dosage stipulated by international regulations [13, 66, 67].

4. CONCLUSIONS

The effect of storage time and temperature on chitosan-based films functionalized with TiO_2 ($CSTiO_2$) and TiO_2-ZnO-MgO (CSTZM) nanoparticles was investigated using FTIR spectroscopy. This is the first report on the structural changes of $CSTiO_2$ and CSTZM films promoted by the storage conditions, to the best of our knowledge. In the chitosan-based films, the main changes during storage were detected in the region from 1700 to 1250 cm^{-1} in a temperature-dependent response, which are associated with changes in the carboxylate group ($–NH_3^+–OOCH$) due to deprotonation of the NH^{3+} groups formed during the development of the film under acetic acidic conditions and to the progressive weakening of the hydrogen bond that involves a dehydration process in the CS-based films. Principal component analysis showed that films stored at ambient temperature showed remarkable structural changes after 7 days compared to the films stored at refrigerated temperatures, which exhibited reduced changes after 21 days of evaluation. Furthermore, there exists a low migration (< 13 %) rate of TiO_2 and TZM from the chitosan matrix to the medium in a temperature-dependent manner. Further studies are needed to correlate the structural changes of $CSTiO_2$ and CSTZM films during storage with their technological and functional properties, which could limit their potential applications.

Acknowledgment. The authors gratefully acknowledge the funding obtained from Tecnologico Nacional de Mexico (No. Grant 10473.21-P). In addition, the authors acknowledge the financial support received as a scholarship to Anaya-Esparza M (702634) from CONACYT-Mexico, and technical support from Ph. D. José Benito Pelayo Vázquez for the use of the FTIR equipment at the "Centro Universitario de Tonalá" of the Universidad de Guadalajara, Jalisco, Mexico.

REFERENCES

[1] L. M. Anaya-Esparza, Z. Villagrán-de la Mora, N. Rodríguez-Barajas, T. Sandoval-Contreras, K. Nuño, D. A. López-de la Mora, A. Pérez-Larios, E. Montalvo-González, Protein–TiO_2: A functional hybrid composite with diversified applications, *Coatings*, **10**, 1194 (2020). DOI: https://doi.org/10.3390/coatings10121194

[2] R. Jovanović-Malinovska, M. Cvetkovska, S. Kuzmanova, C. Tsvetanov, E. Winkelhausen, Immobilization of *Saccharomyces cerevisiae* in novel hydrogels based on hybrid networks of poly(ethylene oxide), alginate and chitosan for ethanol production, *Maced. J. Chem. Chem. Eng*., **29**, 169–179 (2010).

[3] S. H. Mir, L. A. Nagahara, T. Thundat, P. Mokarian-Tabari, H. Furukawa, A. Khosla. Review-Organic-Inorganic hybrid functional materials: An integrated platform for applied technologies, *J. Electrochem. Soc*., **165**, B3137–B3156 (2018). DOI: https://doi.org/10.1149/2.0191808jes

[4] L. M. Anaya-Esparza, Z. Villagrán-de la Mora, J. M. Ruvalcaba-Gómez, R. Romero-Toledo, T. Sandoval-Contreras, S. Aguilera-Aguirre, E. Montalvo-González, A. Pérez-Larios, Use of titanium dioxide (TiO_2) nanoparticles as reinforcement agent of polysaccharide-based materials, *Processes*, **8**, 1395 (2020). DOI: https://doi.org/10.3390/pr8111395

[5] L. M. Anaya-Esparza, J. M. Ruvalcaba-Gómez, C. I. Maytorena-Verdugo, N. González-Silva, R. Romero-Toledo, S. Aguilera-Aguirre, A. Pérez-Larios, E. Montalvo-González. Chitosan-TiO_2: A versatile hybrid composite, *Materials*, **13**, 811 (2020). DOI: 10.3390/ma13040811

[6] B. Tanhaei, A. Z. Moghaddam, A. Ayati, F. Deymeh, M. Sillanpää, Response surface methodology approach for optimization of methyl orange adsorptive removal by magnetic chitosan nanocomposite, *Maced. J. Chem. Chem. Eng*., **36**, 143–151 (2017).

[7] T. P. Ivanovska, L. Petruševska-Tozi, M. D. Kostoska, N. Geškovski, A. Grozdanov, C. Stain, T. Stafilov, K. Mladenovska, Microencapsulation of *Lactobacillus casei* in chitosan-Ca-alginate microparticles using spray-drying method, *Maced. J. Chem. Chem. Eng*., **31**, 115–123 (2012).

[8] N. Todorova, M. Ilarionova, D. Todorov, Antitumor effect of new conjugates of anthracycline antibiotic carcynomicin bound to chitosan, *Maced. J. Chem. Chem. Eng*., **26**, 147–150 (2007).

[9] S. Petrović, L. Rozić, B. Grbić, N. Radić, J. Dostanić, S. Stojadinović, R. Vasilić, Morphology and fractal dimension of TiO_2 thin films, *Maced. J. Chem. Chem. Eng*., **32**, 309–317 (2013).

[10] L. M. Anaya-Esparza, E. Montalvo-González, N. González-Silva, M. D. Méndez-Robles, R. Romero-Toledo, E. M. Yahia, A. Pérez-Larios, Synthesis and characterization of TiO_2-ZnO-MgO mixed oxide and their antibacterial activity, *Materials*, **12**, 698 (2019). DOI: 10.3390/ma12050698

[11] P. Muranyi, C. Schraml, J. Wunderlich, Antimicrobial efficiency of titanium dioxide-coated surfaces, *J. Appl. Microbiol*., **108**, 1966–1973 (2010). DOI: https://doi.org/10.1111/j.1365-2672.2009.04594.x

[12] M. P. Blanco-Vega, M. Hinojosa-Reyes, A. Hernández-Ramírez, J. L. Guzmán-Mar, V. Rodríguez-González, L. Hinojosa-Reyes, Visible light photocatalytic activity of sol-gel Ni doped TiO_2 on p-arsanilic acid degradation, *J. Sol-Gel Sci. Technol*., **85**, 723–731 (2018). DOI: https://doi.org/10.1007/s10971-018-4579-0

[13] H. A. Sharif, A. A. E. Rasha, Z. Al-B. Ramia, Titanium dioxide content in foodstuffs from the Jordanian market: Spectrophotometric evaluation of TiO_2 nanoparticles, *Int. J. Food Res. J.*, **22**, 1024–1029 (2015).

[14] S. S. Behera, U. Das, A. Kumar, A. Bissoyi, A. K. Singh, Chitosan/TiO_2 composite membrane improves proliferation and survival of L929 fibroblast cells: Application in wound dressing and skin regeneration, *Int. J. Biol. Macromol*., **98**, 329–340 (2017). DOI: 10.1016/j.ijbiomac.2017.02.017

[15] U. Siripatrawan, P. Kaewklin, Fabrication and characterization of chitosan-titanium dioxide nanocomposite film as ethylene scavenging and antimicrobial active food packaging, *Food Hydrocoll*., **84**, 125–134 (2018). DOI: https://doi.org/10.1016/j.foodhyd.2018.04.049

[16] S. Wu, J. Kan,X. Dai, X. Shen, K. Zhang, M. Zhu, Ternary carboxymethyl chitosan-hemicellulose-nanosized TiO_2 composite as effective adsorbent for removal of heavy metal contaminants from water, *Fibers Polym*., **18**, 22–32 (2017). DOI: https://doi.org/10.1007/s12221-017-6928-y

[17] L. N. Pincus, F. Melnikov, J. S. Yamani, J. B. Zimmerman, Multifunctional photoactive and selective adsorbent for arsenite and arsenate: Evaluation of nanotitanium dioxide-enabled chitosan cross-linked with copper, *J. Hazard. Mater*., **358**, 145–154 (2018). DOI: https://doi.org/10.1016/j.jhazmat.2018.06.033

[18] A. Chen, G. Zang, G. Chen, X. Hu, M. Yan, S. Guan, C. Shang, L. Lu, Z. Zou, G. Xie, Novel thiourea-modified magnetic ion-imprinted chitosan/TiO_2 composite for simultaneous removal of cadmium and 2,4-dichlorophenol, *Chem. Eng. J*., **191**, 85–94 (2012). DOI: https://doi.org/10.1016/j.cej.2012.02.071

[19] R. Saravanan, J. Aviles, F. Gracia, E. Mosquera, V. K. Gupta, Crystallinity and lowering band gap induced visible light photocatalytic activity of TiO_2/CS (Chitosan) nanocomposites, *Int. J. Biol. Macromol*., **109**, 1239–1245 (2018). DOI: https://doi.org/10.1016/j.ijbiomac.2017.11.125

[20] Y. Haldorai, J. J. Shim, Novel chitosan-TiO_2 nanohybrid: Preparation, characterization, antibacterial, and photocatalytic properties, *Polym. Compos*., **1**, 327–333 (2014). DOI: https://doi.org/10.1002/pc.22665

[21] M. Safari, M. Ghiaci, M. Jafari-Asl, A. A. Ensafi, Nanohybrid organic-inorganic chitosan/dopamine/TiO_2

composites with controlled drug-delivery properties, *Appl. Surf. Sci*., **342**, 26–33 (2015). DOI: https://doi.org/10.1016/j.apsusc.2015.03.028

[22] K. J. Huang, J. Li, Y. Wu, Y. M. Liu, Amperometric immunobiosensor for α-fetoprotein using Au nanoparticles/chitosan/TiO_2–graphene composite based platform, *Biolectrochem*., **90**, 18–23 (2013). DOI: https://doi.org/10.1016/j.bioelechem.2012.10.005

[23] P. Kaewklin, U. Siripatrawan, A. Suwanagul, Y. S. Lee, Active packaging from chitosan-titanium dioxide nanocomposite film for prolonging storage life of tomato fruit, *Biol. Macromol*., **112**, 523–529 (2018). DOI: https://doi.org/10.1016/j.ijbiomac.2018.01.124

[24] L. Qu, G. Chen, S. Dong, Y. Huo, Z. Yin, S. Li, Y. Chen, Improved mechanical and antimicrobial properties of zein/chitosan films by adding highly dispersed nano-TiO_2, *Ind. Crop. Prod.*, **130**, 450–458 (2019). DOI: https://doi.org/10.1016/j.indcrop.2018.12.093

[25] G. Xiao, Y. Zhao, L. Li, J. O. Pratt, H. Su, T. Tan, Facile synthesis of dispersed Ag nanoparticles on chitosan-TiO_2 composites as recyclable nanocatalysts for 4-nitrophenol reduction, *Nanotechnol*., **29**, 1–9 (2018).

[26] L. M. Anaya-Esparza, N. González-Silva, E. M. Yahia, O. A. González-Vargas, E. Montalvo-González, A. Pérez-Larios, Effect of TiO_2-ZnO-MgO mixed oxide on microbial growth and toxicity against *Artemia salina*, *Nanomaterials*, **9**, 992 (2019). DOI: https://doi.org/10.3390/nano9070992

[27] P. Cazón, G. Velázquez, J. A. Ramírez, M. Vázquez, Polysaccharide-based films and coatings for food packaging: A review, *Food Hydrocoll*., **68**, 136–148 (2017). DOI: https://doi.org/10.1016/j.foodhyd.2016.09.009

[28] G. Kerch, V. Korkhov, Effect of storage time and temperature on structure, mechanical and barrier properties of chitosan-based films, *Eur. Food Res. Technol*., **232**, 17–22 (2011). DOI: https://doi.org/10.1007/s00217-010-1356-x

[29] P. Fernández-Saiz, J. M. Lagarón, M. J. Ocio, Optimization of the film-forming and storage conditions of chitosan as an antimicrobial agent, *J. Agric. Food Chem*. **57**, 3298–3307 (2009). DOI: https://doi.org/10.1021/jf8037709

[30] J. Díaz-Visurraga, M. F. Meléndrez, A. García, M. Paulraj, G. Cárdenas, Semitransparent chitosan-TiO_2 nanotubes composite film for food package applications, *J. Appl. Polym. Sci*., **116**, 3503–3515 (2009). DOI: https://doi.org/10.1002/app.31881

[31] H. Yong, X. Wang, R. Bai, Z. Miao, X. Zhang, J. Liu, Development of antioxidant and intelligent pH-sensing packaging films by incorporating purple-fleshed sweet potato extract into chitosan matrix, *Food Hydrocoll*., **90**, 216−224 (2019). DOI: https://doi.org/10.1016/j.foodhyd.2018.12.015

[32] A. E. Wiacek, A. Gozdecka, M. Jurak, Physicochemical characteristics of chitosan-TiO_2 biomaterial. I. Stability and swelling properties, *Ind. Eng. Chem. Res*., **57**, 1859–1870 (2018). DOI: https://doi.org/10.1021/acs.iecr.7b04257

[33] X. Zhang, Y. Liu, H. Yong, Y. Qin, J. Liu, J. Liu, Development of multifunctional food packaging films based on chitosan, TiO_2 nanoparticles and anthocyanin-rich black plum peel extract, *Food Hydrocoll*., **94**, 80–92 (2019). DOI: https://doi.org/10.1016/j.foodhyd.2019.03.009

[34] C. Branca, G. D. Angelo, C. Crupi, K. Khouzami, S. Rifici, G. Ruello, U. Wanderlingh, Role of the OH and NH vibrational groups in polysaccharide nanocomposite interactions: a FTIR-ATR study on chitosan and chitosan/clay films, *Polymer*, **99**, 614–622 (2016). DOI: https://doi.org/10.1016/j.polymer.2016.07.086

[35] S. Hajji, I. Younes, O. Ghorbel-Bellaaj, R. Hajji, M. Rinaudo, M. Nasri, K. Jellouli, Structural differences between chitin and chitosan extracted from three different marine sources, *Int. J. Biol. Macromol*., **65**, 298–306 (2014). DOI: https://doi.org/10.1016/j.ijbiomac.2014.01.045

[36] D. Timotious, Y. Kusumastuti, N. A. C. Imani, Rochmadi, N. R. E. Putri, S. S. Rahayu, S. K. Wirawan, M. Ikawati, Kinetics of drug release profile from maleic anhydride-grafted chitosan film, *Matter. Res. Exp*., **7**, 046403 (2020). DOI: https://doi.org/10.1088/2053-1591/ab80d9

[37] T. Lefevre, M. Subirade, M. Pézolet, Molecular descriptionof the formation and structure of plasticized globular protein films, *Biomacromol*., **6**, 3209–3219 (2005). DOI: https://doi.org/10.1021/bm050540u

[38] K. A. M. Amin, M. I. H. Panhius, Reinforced materials based on chitosan, TiO_2 and Ag composites, *Polymers* **4**, 590–599 (2012). DOI: https://doi.org/10.3390/polym4010590

[39] W. Li, K. Zheng, H. Chen, S. Feng, W. Wang, C. Qin, Influence of nanotitanium dioxide and clove oil on chitosan-starch film characteristics, *Polymers* **11**, 1418 (2019). DOI: https://doi.org/10.3390/polym11091418

[40] M. Taspika, R. W. Desiati, M. Mahardika, E. Sugiarti, H. Abral, Influence of TiO_2/Ag particles on the properties of chitosan film, *Adv. Nat. Sci. Nanosci. Nanotechnol*., **11**, 015017 (2020). DOI: https://doi.org/10.1088/2043-6254/ab790e

[41] T. Ikhlef-Taguelmimt, A. Hamiche, I. Yahiaoui, T. Bendellali, H. Lebik-Elhadi, H. Ait-Amar, F. Aissani-Benissad, Tetracycline hydrochloride degradation by heterogeneous photocatalysis using TiO_2(P25) immobilized in biopolymer (Chitosan) under UV irradiation, *Water Sci. Technol*., **82**, 1570–1578 (2020). DOI: https://doi.org/10.2166/wst.2020.432

[42] F. H. A. El-Kader, A. M. Shehap, A. A. Bakr, O.T. Hussain, Characterization of clay/chitosan nanocomposites and their use for adsorption on Mn(II) from aqueous solution, *Int. J. Sci. Eng. Appl*., **4**, 174–185 (2015). DOI: 10.7753/ijsea0404.1004

[43] L. Zhang, W. Xia, X. Liu, W. Zhang, Synthesis of titanium cross-linked chitosan composite for efficient adsorption and detoxification of hexavalent chromium from water, *J. Mater. Chem. A*. **3**, 331–340 (2015). DOI: https://doi.org/10.1039/C4TA05194G

[44] Q. Xiao, X. Gu, S. Tan, Drying process of sodium alginate films studied by two-dimensional correlation ATR-FTIR spectroscopy, *Food Chem*., **164**, 179–184 (2014). DOI: https://doi.org/10.1016/j.foodchem.2014.05.044

[45] S. Afzal, E. M. Samsudin, L. K. Mun, N. M. Julkapli, S. B. A. Hamid, Room temperature synthesis of TiO_2 sup-

ported chitosan photocatalyst: Study on physicochemical and adsorption photo-decolorization properties, *Mater. Res. Bull.*, **86**, 24–29 (2017).
DOI: https://doi.org/10.1016/j.materresbull.2016.09.028

[46] S. A. Oleyaei, Y. Zahedi, B. Ghanbarzadeh, A. A. Moayedi, Modification of physicochemical and thermal properties of starch films by incorporation of TiO_2 nanoparticles, *Int. J. Biol. Macromol*., **89**, 256–264 (2016).
DOI: https://doi.org/10.1016/j.ijbiomac.2016.04.078

[47] D. Arikal, A. Kallingal, Photocatalytic degradation of azo and anthraquinone dye using TiO_2/MgO nanocomposite immobilized chitosan hydrogels, *Environ. Technol*., **1**, 1–14 (2019).
DOI: https://doi.org/10.1080/09593330.2019.1701094

[48] J. Vidic, S. Stankic, F. Haque, D. Ciric, R. Le Goffic, A. Vidy, J. Jullipe, B. Delmas, Selective antibacterial effects of mixed ZnMgO nanoparticles, *J. Nanopat. Res*., **15**, 1595 (2013).
DOI: https://doi.org/10.1007/s11051-013-1595-4

[49] H. Zhu, R. Jiang, Y. Fu, Y. Guan, J. Yao, L. Xiao, G. Zeng, Effective photocatalytic decolorization of methyl orange utilizing TiO_2/ZnO/chitosan nanocomposite films under simulated solar irradiation, *Desalination*, **286**, 41–48 (2012).
DOI: https://doi.org/10.1016/j.desal.2011.10.036

[50] X. Wei, Q. Li, H. Hao, H. Yang, Y. Li, T. Sun, X. Li, Preparation, physicochemical and preservation properties of Ti/ZnO/in situ SiOx chitosan composite coatings, *J. Sci. Food Agric*., **100**, 570–577 (2020).
DOI: https://doi.org/10.1002/jsfa.10048

[51] B. D. Malhorta, A. Kaushik, Metal oxide-chitosan based nanocomposite for cholesterol biosensor, *Thin Solid Films*, **518**, 614–620 (2009).
DOI: https://doi.org/10.1016/j.tsf.2009.07.036

[52] Z. Osman, A. K. Arof, FTIR studies of chitosan acetate based polymer electrolytes, *Electrochim. Acta*, **48**, 993–999 (2003).
DOI: https://doi.org/10.1016/S0013-4686(02)00812-5

[53] H. M. Kam, E. Khor, L.Y. Lim, Storage of partially deacetylated chitosan films, *J. Biomed. Mater. Res*., 1999, **48**, 881–888 (2002).
DOI:https://doi.org/10.1002/(SICI)1097-4636(1999)48:6<881::AID-JBM18>3.0.CO;2-2

[54] A. A. Mejenom, M. N. Hafiza, M. I. N. Isa, X-ray diffraction and infrared spectroscopic analysis of solid biopolymer electrolytes based on dual blend carboxymethyl cellulose-chitosan doped with ammonium bromide, *ASM Sci. J*., **1**, 37–46 (2018).

[55] G. Lawrie, I. Keen, B. Drew, A. Chandler-Temple, L. Rintoul, P. Fredericks, L. Grondahl, Interactions between alginate and chitosan biopolymers characterized using FTIR and XPS, *Biomacromol.*, **8**, 2533–2541 (2007). DOI: https://doi.org/10.1021/bm070014y

[56] S. Rivero, L. Damonte, M. A. García, A. Pinotti, An insight into the role of glycerol in chitosan films. *Food Biophys*., **11**, 117–127 (2016).
DOI: https://doi.org/10.1007/s11483-015-9421-4

[57] J. A. González-Calderon, J. Vallejo-Montesinos, H. N. Martíez-Martínez, R. Cerecero-Enríquez, L. López-Zamora, Effect of chemical modification of titanium dioxide particles via silanization under properties of chitosan/potato-starch films, *Mex. J. Chem. Eng*., **18**, 913–927 (2019).
DOI:https://doi.org/10.24275/uam/izt/dcbi/revmexingquim/2019v18n3/GonzalezC

[58] M. Stevanović, M. Djošić, A. Janković, V. Kojić, M. Vukasinović-Sekulić, J. Stojanović, J. Odović, M. C. Sakač, R. K. Yop, V. Misković-Stanković, Antibacterial graphene-based hydroxyapatite/chitosan coating with gentamicin for potential applications in bone tissue engineering, *J. Biomed. Mater. Res*., **108**, 2175–2189 (2020). DOI: https://doi.org/10.1002/jbm.a.36974

[59] K. K. Dash, N. A. Ali, D. Das, D. Mohanta, Thorough evaluation of sweet potato starch and lemon-waste pectin based-edible films with nano-titania inclusions for food packaging applications, *Int. J. Biol. Macromol*., **139**, 449–458 (2019).
DOI: https://doi.org/10.1016/j.ijbiomac.2019.07.193

[60] A. Yamamoto, J. Kawada, T. Yui, K. Ogawa, Conformational behavior of chitosan in the acetate salt: An X-ray study, *Biosci. Biotechnol. Biochem*., **61**, 1230–1232 (1997). DOI: https://doi.org/10.1271/bbb.61.1230

[61] N. M. Vicentini, N. Dupuy, M. Leitzelman, M. P. Cereda, P. J. A. Sobral, Prediction of cassava starch edible film properties by chemometric analysis of infrared spectra, *Spectrosc. Lett. Int. J. Rapid Commun*., **38**, 749–767 (2005).
DOI: http://dx.doi.org/10.1080/00387010500316080

[62] H. H. A. Sherif, S. K. H. Khalil, A. G. Hegazi, W. A. Khalil, M. A. Moharram, Factors affecting the antibacterial activity of chitosan-silver nanocomposite, *IET Nanobiotechnol*., **11**, 731–737 (2017).
DOI: 10.1049/iet-nbt.2016.0249

[63] J. T. Martins, M. A. Cerqueira, A. I. Bourbon, A. C. Pinheiro, B. W. S. Souza, A. A. Vicente, Synergistic effects between κ-carrageenan and locust bean gum on physicochemical properties of edible films made thereof, *Food Hydrocoll*., **29**, 280–289 (2012).
DOI: https://doi.org/10.1016/j.foodhyd.2012.03.004

[64] J. M. Lagarón, P. Fernández-Saiz, M. J. Ocio, Using ATR-FTIR spectroscopy to design active antimicrobial food packaging structures based on high molecular weight chitosan polysaccharide, *J. Agric. Food Chem*., **55**, 2554–2562 (2007).
DOI: https://doi.org/10.1021/jf063110j

[65] Z. Lian, Y. Zhang, Y. Zhao, Nano-TiO_2 particles and high hydrostatic pressure treatment for improving functionality of polyvinyl alcohol and chitosan composite films and nano-TiO_2 migration from film matrix in food simulants, *Innov. Food Sci. Emerg. Technol*., **33**, 145–153 (2016).
DOI: https://doi.org/10.1016/j.ifset.2015.10.008

[66] M. P. Paarakh, P. A. Jose, C. M. Setty, G. V. P. Christoper, Release kinetics-concepts and applications, *Int. J. Pharm. Res. Technol*., **8**, 12–20 (2018).

[67] M. Alizadeh-Sani, E. Mohammadian, D. J. McClements, Eco-friendly active packaging consisting of nanostructured biopolymer matrix reinforced with TiO_2 and essential oil: Application for preservation of refrigerated meat, *Food Chem.*, **322**, 126782 (2020).
DOI: https://doi.org/10.1016/j.foodchem.2020.126782